

# Pore Environment Control and Enhanced Performance of Enzymes Infiltrated in Covalent Organic Frameworks

Qi Sun,<sup>†,||</sup> Chung-Wei Fu,<sup>†,‡,||</sup> Briana Aguila,<sup>†</sup> Jason Perman,<sup>†</sup> Sai Wang,<sup>§</sup> Hsi-Ya Huang,<sup>\*,‡,||</sup> Feng-Shou Xiao,<sup>§</sup> and Shengqian Ma<sup>\*,†</sup>

<sup>†</sup>Department of Chemistry, University of South Florida, 4202 E. Fowler Avenue, Tampa, Florida 33620, United States

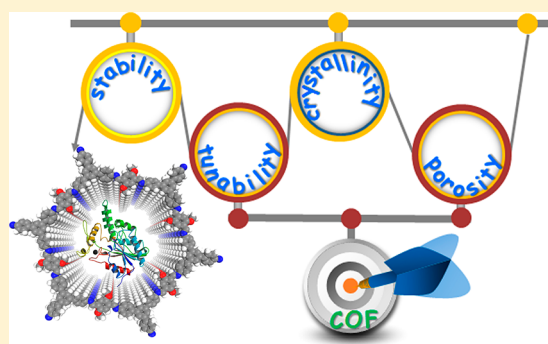
<sup>‡</sup>Chung Yuan Christian University 200, Chung-Pei Road, Chung-Li 32023, Taiwan Republic of China

<sup>§</sup>Key Laboratory of Applied Chemistry of Zhejiang Province and Department of Chemistry, Zhejiang University, Hangzhou 310028, P. R. China

## Supporting Information

**ABSTRACT:** In the drive toward green and sustainable methodologies for chemicals manufacturing, biocatalysts are predicted to have much to offer in the years to come. That being said, their practical applications are often hampered by a lack of long-term operational stability, limited operating range, and a low recyclability for the enzymes utilized. Herein, we show how covalent organic frameworks (COFs) possess all the necessary requirements needed to serve as ideal host materials for enzymes. The resultant biocomposites of this study have shown the ability boost the stability and robustness of the enzyme in question, namely lipase PS, while also displaying activities far outperforming the free enzyme and biocomposites made from other types of porous materials, such as mesoporous silica and metal–organic frameworks, exemplified in the kinetic resolution of the alcohol assays performed.

The ability to easily tune the pore environment of a COF using monomers bearing specific functional groups can improve its compatibility with a given enzyme. As a result, the orientation of the enzyme active site can be modulated through designed interactions between both components, thus improving the enzymatic activity of the biocomposites. Moreover, in comparison with their amorphous analogues, the well-defined COF pore channels not only make the accommodated enzymes more accessible to the reagents but also serve as stronger shields to safeguard the enzymes from deactivation, as evidenced by superior activities and tolerance to harsh environments. The amenability of COFs, along with our increasing understanding of the design rules for stabilizing enzymes in an accessible fashion, gives great promise for providing “off the shelf” biocatalysts for synthetic transformations.



## INTRODUCTION

Cell-free enzyme catalysis has not found widespread industrial adoption, despite decades of active research, because the challenges associated with the durability and turnover outweigh the touted advantages of replacing enzymes with synthetic catalysts.<sup>1</sup> Coupling enzymes with solid supports afford a unique opportunity to shield them from deactivation, provide potential for recyclability, and increase the operational stability. This is achieved by taking advantage of the chemical and mechanical properties of the host materials.<sup>2</sup> Among various developed strategies for enzyme immobilization, infiltration within pores holds great promise, on account of the mild operating conditions, whereby the entrapped enzymes undergo minimal chemical modifications, leaving intact the enzymatic structure to maintain its activity.<sup>3</sup>

Significant efforts have been made to develop advanced materials for encapsulating enzymes in a stable and convenient manner for use in enzymatic catalysis.<sup>4</sup> A range of porous supports, such as Celite, zeolites, and mesoporous silica, have

been investigated in the quest for the optimal performance of immobilized enzymes.<sup>5</sup> However, the lack of functionality of these materials for providing specific interactions with enzymes remains a frontier issue. Recently, metal–organic frameworks (MOFs) have been gaining popularity as vectors for enzyme immobilization, due to their remarkable structural/chemical design variety as well as their unparalleled surface tunability.<sup>6</sup> In spite of these notable advantages, the issues associated with their long-term water/chemical stability and the potential leaching of unwanted toxic metal ions have to be addressed to achieve the desired enzyme-MOF composite.<sup>7</sup> Therefore, the development of alternative host materials is imperative for targeting both high enzyme loading and enhanced stability. Materials featuring no metal ions, high chemical stability, functional modularity, and long-range order are highly desirable.

Received: October 5, 2017

Published: December 25, 2017

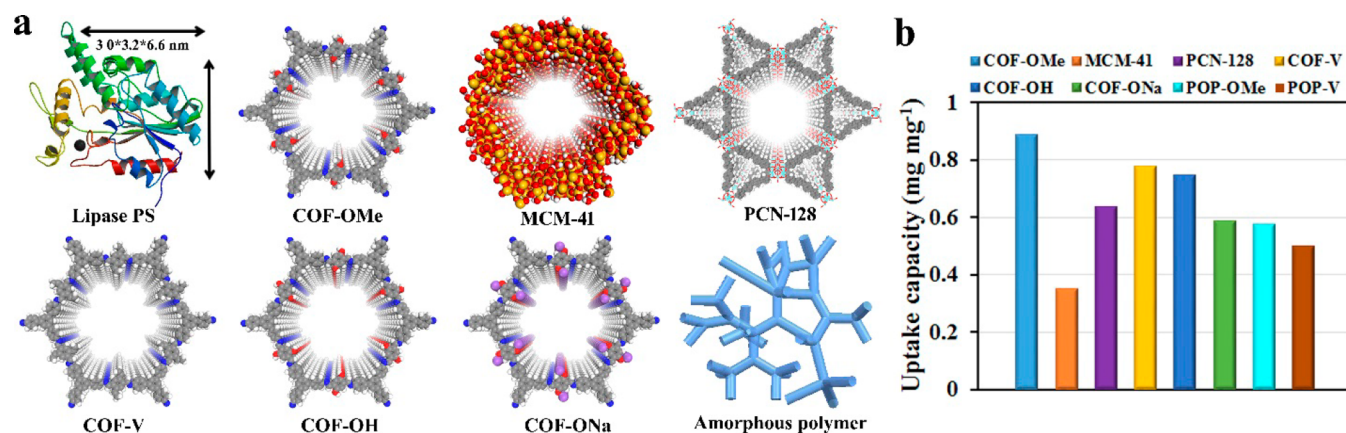


**Figure 1.** (a) Graphic view of lipase PS and porous materials used for the immobilization of enzymes (blue, N; gray, C; red, O; white, H; yellow, Si; purple, Na). (b) Enzyme uptake capacity of various porous materials after incubation in lipase PS solution ( $30 \text{ mg mL}^{-1}$ ) for 6 h (see also Table S1).

Covalent organic frameworks (COFs), built by strong organic covalent bonds in a periodic arrangement entirely from light elements (i.e., H, B, C, N, and O), have exploded as a new area of materials research in the past decade.<sup>8</sup> The inherently low density and high surface area of many COFs, along with their crystallinity, lends themselves as intriguing materials for a plethora of potential applications pertaining to gas storage/separation,<sup>9</sup> catalysis,<sup>10</sup> optoelectronics,<sup>11</sup> proton conduction,<sup>12</sup> environmental remediation,<sup>13</sup> and many more.<sup>14</sup> We postulate that COFs present an attractive category of host matrix candidates, which combine key features relevant to enzyme immobilization, namely tunability, porosity, crystallinity, and stability. With their customizable composition, the functional groups on their surfaces can be readily tailored to favor specific interactions between COFs and enzymes, thereby enabling the modulation of enzymatic activity to be rigorously controlled. In addition, COFs provide continuous and confined open channels at the nanoscale, affording an accessible high surface area interface for infiltrating enzymes and pathways for allowing rapid transportation of reagents, while the well-defined and relatively small pore size impedes the aggregation of enzymes. Moreover, the structural robustness of COFs represents an important attribute in comparison with most of their MOF analogues.

In view of enzymatic catalysis, lipases constitute one of the most useful moieties in the current scenario of biocatalysis. This is due in part to their commercial availability and versatile catalytic behavior, showing exceptional performance in a variety of reactions.<sup>15</sup> Nonetheless, they also suffer from low stability and lack of recyclability.<sup>16</sup> For these reasons, lipases are the enzyme of choice for this proof-of-concept study. We show herein that mesoporous COFs possess all the necessary traits to be promising host frameworks for infiltration of enzymes. This is demonstrated by a significant enhancement of the native enzymatic performance as well as the additional benefits of recyclability and resistance to a wide range of environmental/industrial conditions. The immobilized enzyme was characterized by its superior performance compared to the free enzyme and to methods utilizing other types of related porous materials such as MOFs (PCN-128y) and mesoporous silica (MCM-41). In addition, to reveal the role of the long-range order porous structure of COFs, amorphous polymers with the same composition were employed as host matrices. These gave rise to inferior performance compared to that of the COFs in terms of both enzyme uptake capacity and catalytic activity.

Furthermore, COFs with the same reticular yet different functionalities were compared. This was to show that the customizable surface characteristics are well suited to create a stabilizing microenvironment for enzymes through designed host–guest interactions. These findings suggest design rules of host frameworks in enzyme-immobilization applications.

## RESULTS AND DISCUSSION

**Materials Preparation, Physicochemical Characterization, and Enzyme Uptake Capacity Evaluation.** To carry out this study, TPB-DMTP-COF (hereafter denoted as COF-OMe), synthesized by the condensation between dimethoxyterephthalaldehyde (DMTP) and 1,3,5-tris(4-aminophenyl)benzene (TPB), was initially chosen as a host material, due to its extraordinary stability, high surface area, and ordered one-dimensional (1D) channel-like pores (Figures 1a and S1).<sup>17</sup> We reasoned that the large mesoporous channels of COF-OMe (3.3 nm) should be suitable for confining but not constricting Amano lipase PS (from *Burkholderia cepacia*), a protein ( $3.0 \text{ nm} \times 3.2 \text{ nm} \times 6.0 \text{ nm}$ ) featuring a small-axis length of  $\sim 3.2 \text{ nm}$  (Figure 1a). To immobilize the enzyme, COF-OMe was treated with a phosphate buffer solution of lipase PS ( $30 \text{ mg mL}^{-1}$ , pH = 7.0) at room temperature. The resultant material was then washed with water two times to remove the loosely adsorbed lipase PS species on the surface, affording the composite denoted as lipase@COF-OMe. The uptake capacity of lipase PS by COF-OMe was obtained via a bicinchoninic acid (BCA) assay using UV–vis spectroscopy to detect the concentration of lipase PS in the original solution as well as the combination of the supernatant and washing solutions after immobilization (see details in the Supporting Information). An equilibrium uptake of  $0.95 \text{ mg mg}^{-1}$  (average of three individual batches) was reached within 6 h. To validate the UV–vis results, elemental analysis was performed. Based on the N element content before and after infiltration of lipase PS, the enzyme uptake was calculated to be  $0.89 \text{ mg mg}^{-1}$ , which is consistent with that of the UV–vis results. In addition, lipase@COF-OMe showed an extra FT-IR peak at  $1648 \text{ cm}^{-1}$  in comparison with pristine COF-OMe, which was associated with the amide groups of the enzyme (Figure S2),<sup>18</sup> thus confirming the enzyme incorporation. The overall morphology of COF-OMe remained unchanged after the enzyme infiltration as revealed by the SEM images (Figure S3). EDX mapping showed the homogeneous distribution of N, S, and O elements in lipase@

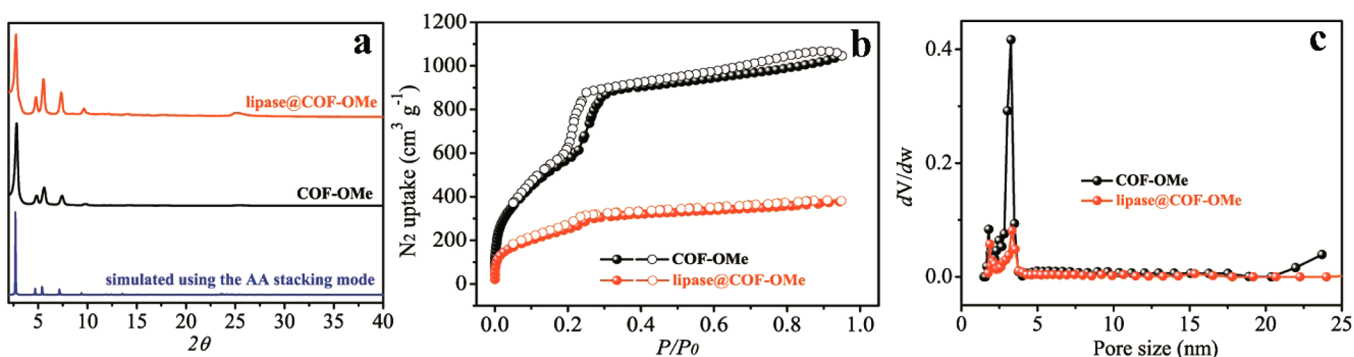


**Figure 2.** (a) Simulated and experimental PXRD patterns and (b, c)  $N_2$  sorption isotherms collected at 77 K and corresponding pore size distribution based on the nonlocal density functional theory method.

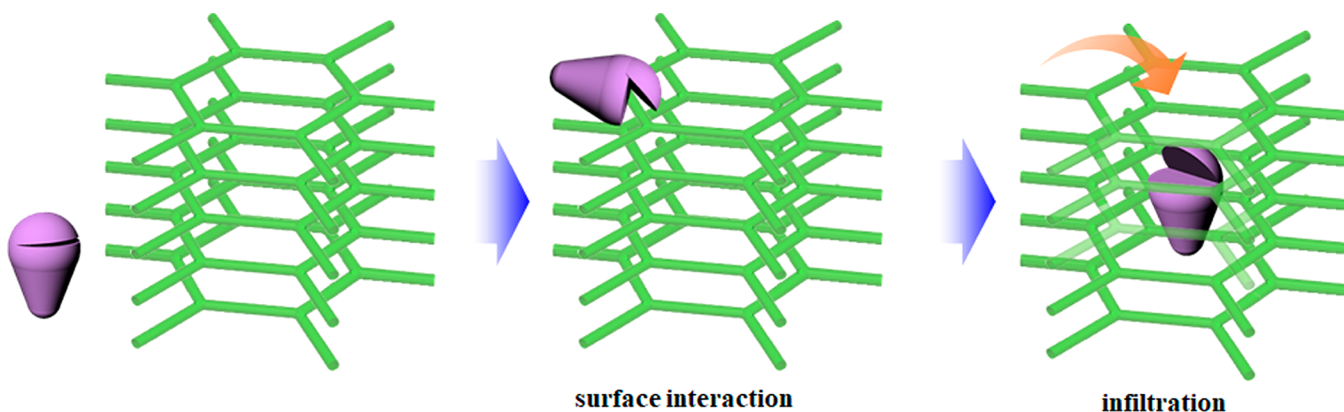


**Figure 3.** Schematic illustration of the translocation of enzyme into the pore channels.

COF-OMe (Figure S4). To further determine the distribution of lipase PS in the resultant composite, fluorescent probe fluorescein isothiocyanate (FITC) was used to label the enzyme molecules. From the confocal laser scanning microscopy (CLSM), it can be observed that FITC-lipase PS (green) is present throughout lipase@COF-OMe, thereby providing a clear demonstration that the enzyme homogeneously accommodates in the crystalline framework (Figure S5).

Powder X-ray diffraction (PXRD) patterns verified that the crystalline structure of COF-OMe was retained after enzyme encapsulation. However, the relative intensity of the first peak corresponding to the (100) peak decreased, which can be presumably attributed to the presence of a multitude of flexible enzymes situated in the pores of COF-OMe, which weakens the diffractions (Figure 2a).<sup>13a</sup> Nitrogen sorption isotherms measured at 77 K indicate that the BET surface area of COF-OMe decreases from  $1740 \text{ m}^2 \text{ g}^{-1}$  to  $784 \text{ m}^2 \text{ g}^{-1}$  after entrapment of lipase (Figure 2b). The density functional theory pore-size distribution analyses of COF-OMe and lipase@COF-OMe showed that both of the samples have a pore size centered at 3.3 nm (Figure 2c), whereas the pore volume corresponding to the hexagonal channels dropped from  $1.62 \text{ cm}^3 \text{ g}^{-1}$  to  $0.59 \text{ cm}^3 \text{ g}^{-1}$  after lipase PS encapsulation. These results are consistent with the contention that a considerable portion of the enzyme occupies within the pore channels. Albeit the pores of the COF are partially occupied by the enzymes, the surface area of the biocomposite is still impressive, and the remaining pore volume and apertures of the COF can enable the reactants to readily access the enzymes situated in the pore channels. Together, these results suggest that COFs

may serve as a promising alternative platform for enzyme infiltration.

It is well-known that protein migration into the pores of materials is initiated by surface contacts,<sup>19</sup> reminiscent of that seen in biological mechanisms associated with protein transport through membranes (Figure 3). In this sense, the pore environment of the host matrix is of essential importance, given that the pore surface forms a microscopic interface with guest molecules. Therefore, varying forces are in effect during the uptake as well as the consequential catalytic performance.

To investigate the effect of pore surface properties as a result of varying host matrices' composition on the enzyme uptake, two other representative types of porous materials were selected for comparison. One is an inorganic material, mesoporous silica MCM-41 with a two-dimensional hexagonal pore structure (pore diameter ca. 40 Å, BET =  $1008 \text{ m}^2 \text{ g}^{-1}$ , Figures 1a and S6).<sup>20</sup> The other is an organic-inorganic hybrid material, mesoporous MOF PCN-128y (Zr) containing two types of 1D channels, a hexagonal channel with a diameter of 4.3 nm and a triangular channel with a diameter of 1.5 nm (BET =  $2680 \text{ m}^2 \text{ g}^{-1}$ , Figures 1a and S7).<sup>21</sup> As shown in Figure 1b, they gave rise to lipase PS uptake capacities of 0.35 and 0.64  $\text{mg mg}^{-1}$ , respectively, after incubating in the  $30 \text{ mg mL}^{-1}$  lipase PS stock solution for 6 h (a prolonged adsorption time did not yield obvious improvements), thereby suggesting that COFs act as favorable candidates for lipase immobilization in view of uptake capacity. To further illustrate the benefit of using COFs as a platform for accommodating enzymes, the performance of another COF material (COF-V, BET =  $1150 \text{ m}^2 \text{ g}^{-1}$ , Figures 1a and S8–S10)<sup>13a</sup> which is isostructural to COF-OMe, synthesized by the condensation of 1,3,5-tris(4-

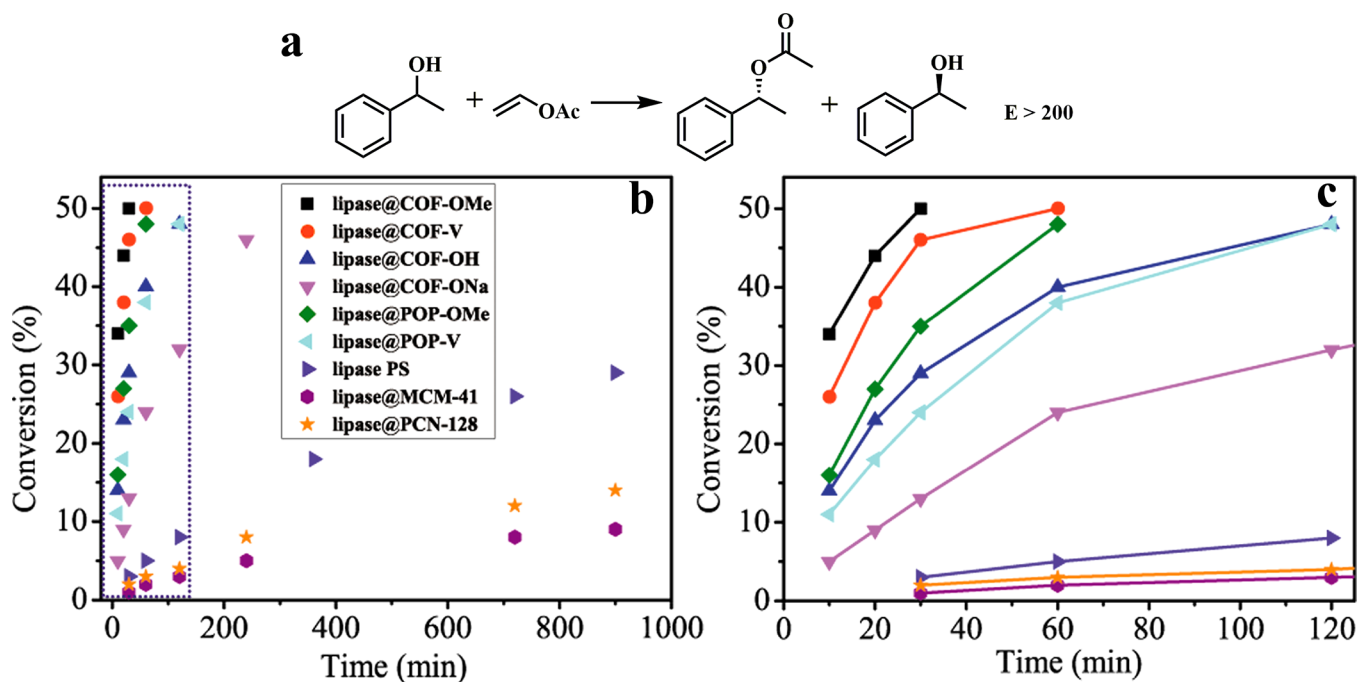


**Figure 4.** Catalytic performance comparison of various biocomposites. (a) Reaction equation. (b) Plots of conversion of kinetic resolution of 1-phenylethanol with vinyl acetate as the acyl donor over various lipase PS infiltrated porous materials. (c) Enlarged section of blue rectangle in A (lines are guidelines for the eyes). Reaction conditions: 1-phenylethanol (0.25 mmol), vinyl acetate (0.75 mmol), hexane (1.2 mL), catalyst (2.5 mg), and 45 °C.

aminophenyl)benzene and 2,5-divinylterephthalaldehyde, was evaluated. Under identical conditions, COF-V showed a lipase PS uptake capacity of  $0.78 \text{ mg mg}^{-1}$ , which is slightly inferior to that of COF-OMe, ascribed to the lower surface area, but outperforms that of MCM-41 and PCN-128y. These porous materials have comparable aperture sizes and ordered pore structures, together with MCM-41 and COF-V exhibiting similar surface areas, yet MCM-41 affords half the uptake amount of COF-V, whereas PCN-128y with much higher surface area compared with other materials tested does not show high adsorption performance. Taking this into account we deduce that rather than the textural features, the different chemical compositions of these materials seem to be responsible for the distinct disparity in enzyme loading. Different pore surface environments of host matrices result in diverse host–guest interactions, and therefore different adsorption mechanisms are likely involved in various adsorbents for enzyme uptake. Notably, in addition to hydrogen-bonding and van der Waals forces, which exist in all cases among the materials tested, COF-OMe and COF-V are expected to have hydrophobic–hydrophobic interactions with lipase PS.

To gain better insight into the effect of pore hydrophobicity on the enzyme uptake, two isorecticular structures to COF-OMe with hydrophilic properties were prepared for comparison (COF-OH and COF-ONa, see Figure S11 water contact angle results). COF-OH (BET =  $1620 \text{ m}^2 \text{ g}^{-1}$ , Figures 1a and S12–S14) was obtained by the condensation of 1,3,5-tris(4-aminophenyl)benzene and 2,5-dihydroxyterephthalaldehyde,<sup>14b</sup> and further treatment of COF-OH with a NaOH aqueous solution yielded COF-ONa (BET =  $1492 \text{ m}^2 \text{ g}^{-1}$ , Figures 1a and S15–S17). COF-OH and COF-ONa exhibited lipase PS uptake capacities of  $0.75$  and  $0.59 \text{ mg mg}^{-1}$ , respectively, which are lower than both COF-OMe and COF-V. Given the

similarity of pore structures and the importance of hydrophobicity over surface area (comparison among COF-V, COF-OH, and COF-ONa), these results support the hypothesis that the hydrophobic pore environment is favorable for the infiltration of lipase PS.

Apart from the surface properties, the uniform open-pore structure may also be propitious for enzyme immobilization. To investigate the role of the ordered 1D channel in the encapsulation of guest molecules, an amorphous analogue of COF-OMe was synthesized by the condensation between dimethoxyterephthalaldehyde and 1,3,5-tris(4-aminophenyl)benzene in DMSO. The resultant material (POP-OMe, BET:  $1056 \text{ m}^2 \text{ g}^{-1}$ , Figures S18 and S19) gave an enzyme uptake of  $0.58 \text{ mg mg}^{-1}$ , only 65% of that achieved by employing COF-OMe. The same trend was also found in the case of COF-V and its amorphous analogue POP-V ( $0.78 \text{ mg mg}^{-1}$  vs  $0.50 \text{ mg mg}^{-1}$ , Figures S20 and S21). It is therefore indicated that the disordered and discontinued pore channels significantly compromise the uptake capacity, demonstrating the great advantage of the rigid and uniformly open porous COFs over amorphous porous polymers.

Interpreting these results, it is sufficiently concluded that the ordered hydrophobic pore channels show considerable potential for high lipase PS loading, provided that (1) the hydrophobic environment gives an impetus to drive the enzyme in buffer aqueous solutions into the pore channels and provides a high affinity for protein molecules, and (2) the ordered channels afford ideal room for the enzyme to be “comfortably” hosted, which may affect the accessibility of the enzyme and thereby its activity. Therefore, the intrinsic hydrophobicity of the majority of COFs as a result of their compositions and crystallinity makes them stand out from other porous materials for lipase immobilization.

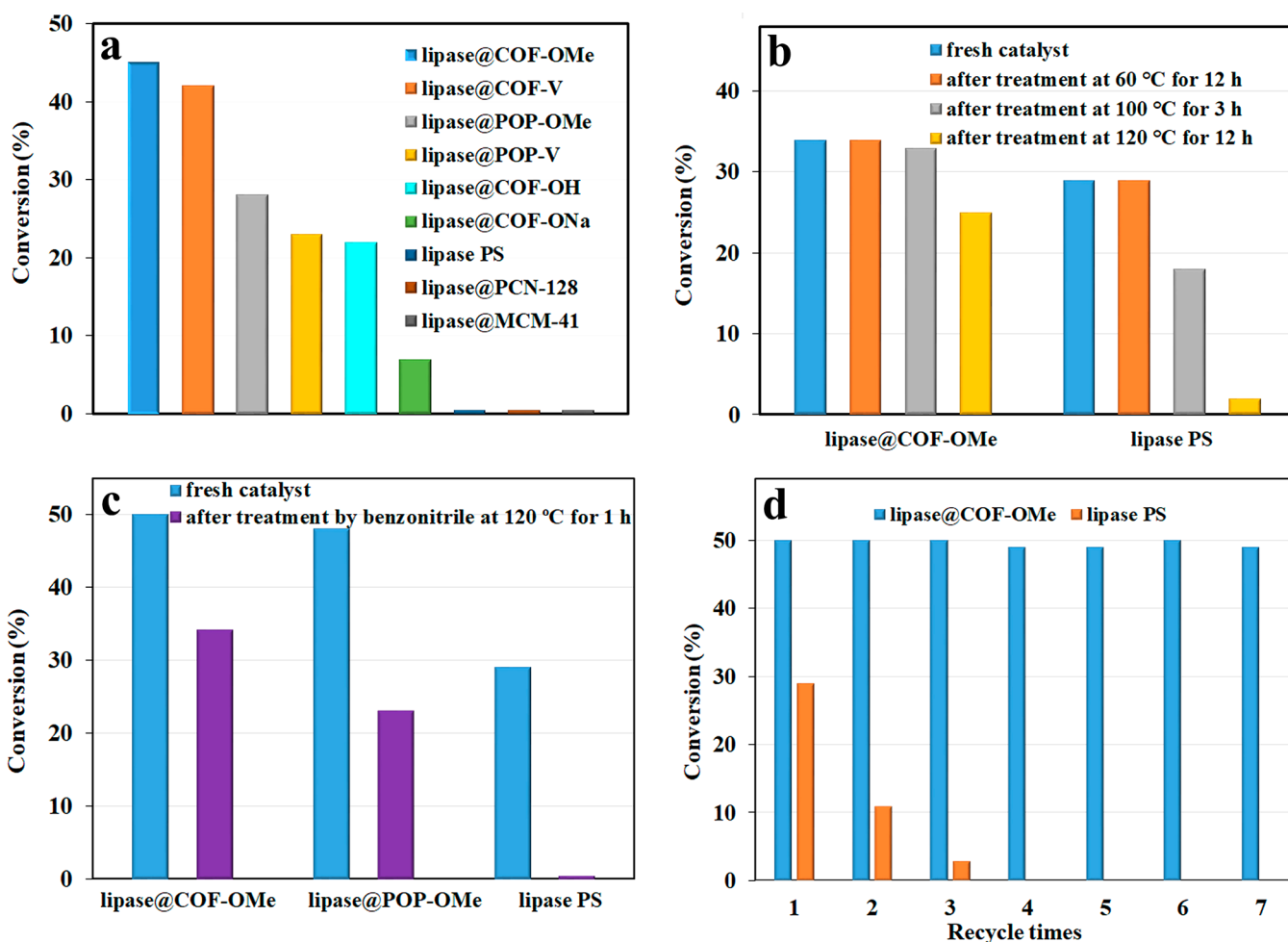


**Figure 5.** (a) Enzymatic activity assays in the kinetic resolution of 1-phenylethanol with vinyl acetate using acetonitrile as the solvent. (b and c) The retention of enzymatic activities after treatment under various conditions. (d) Recycling tests of lipase@COF-OMe and free lipase PS. Reaction conditions: 1-phenylethanol (0.25 mmol), vinyl acetate (0.75 mmol), hexane (1.2 mL), catalyst (2.5 mg), and 45 °C.

**Enzymatic Activity Assay.** Given the importance of enantiomerically pure alcohols and the highly enantioselective resolution activity of lipases, the kinetic resolution of racemic 1-phenylethanol with vinyl acetate as the acyl donor was chosen as a representative reaction to determine the effect of surface properties and pore architecture of the host materials on the activity of encapsulated enzymes.<sup>22</sup> Considering that lipase PS is characterized by superior performance upon exposure to nonpolar organic solvents, reactions were performed using hexane as the medium with 1-phenylethanol and vinyl acetate in the presence of the same amount of biocomposites (2.5 mg). For comparison, the activity of free lipase PS was also evaluated. It is worth mentioning that there is only one conformation product detected for all the lipase PS-involved catalytic systems (Figure S22). Time-dependent 1-phenylethyl acetate yields were monitored (no product was detected in the absence of lipase PS), and only 3% conversion of 1-phenylethanol was observed for free lipase PS (2.5 mg) after 30 min. Prolonging the reaction time to 15 h, a 29% 1-phenylethyl acetate yield was achieved. In sharp contrast, lipase@COF-OMe and lipase@COF-V exhibited 34% and 26% conversions of 1-phenylethanol, respectively, after 10 min, and both of the catalytic systems afforded higher than 49% conversion within 30 min (the theoretical yield is 50%), placing them among the best catalysts (Table S2). It is

interesting to note that the enzymatic performance was compromised with increasing hydrophilicity of the COF materials, but their activities are still impressive. Lipase@COF-OH and lipase@COF-ONa provided 1-phenylethyl acetate yields of 29% and 13%, respectively, after 30 min, which far outperforms that of the free enzyme. Under identical conditions, lipase@MCM-41 and lipase@PCN-128y showed unsatisfactory activities, giving rise to 9% and 14% conversions of 1-phenylethanol after 15 h, respectively, much inferior to that of free lipase PS and all the COF-based biocomposites (Figure 4). The huge discrepancy in enzymatic activities of the catalytic systems tested is likely caused by two reasons, different lipase loading and a possible change of the enzyme conformation after immobilization due to different host-guest interactions involved. In this context, to exclude the catalytic performance difference as a result of enzyme loading, a biocomposite with a lower lipase loading amount was synthesized by incubation of COF-OMe in a 10 mg mL<sup>-1</sup> lipase phosphate buffer aqueous solution to yield a catalyst with a lipase PS loading amount of 0.21 mg g<sup>-1</sup>. Again, the COF host material favored superior activity, and a 38% conversion of 1-phenylethanol was observed after 30 min. Given that the trend of activities is unparalleled to that of enzyme loading, this suggests that the pore environment of the host materials has an important effect on the performance of the encapsulated

enzymes. Most lipases show interfacial activation, where an amphiphilic  $\alpha$ -helical loop, or “lid”, covering the active site of the lipase in the native state (close state), will roll back and bring full access to the catalytic triad (open state), therefore resulting in a remarkably increased enzymatic activity. Adsorption of lipases on hydrophobic supports is thought to mimic this interfacial activation, facilitating the opening of the hydrophobic lid and thus activation of the enzyme.<sup>23a</sup> The hydrophobic character of COF-OMe and COF-V, which allow for strong interactions between the hydrophobic groups surrounding the entrance of the active site of the enzyme and the support surface, accounts for the observed exceptionally high activities (Figure 3). In contrast, when lipase PS is anchored on the hydrophilic support, the lid would shield the active site from the substrates as in the native state, thus producing a depressed activity.<sup>23</sup> To provide proof, FT-IR analysis of lipase@COF-OMe and lipase@MCM-41 was performed (Figure S23). The free lipase PS and lipase@MCM-41 show similar amide I bands at approximately 1642  $\text{cm}^{-1}$ , arising from a C=O stretching vibration coupled with an out-of-phase C–N stretching, and C–C–N deformation of the peptide backbone. On the contrary, lipase@COF-OMe exhibits an obvious shift of the amide I band to a higher wavenumber (1679  $\text{cm}^{-1}$ ), implying a different conformation of lipase in this material, which can be explained by a structural transition of the entrapped protein to the open-lid or the enzymatic active conformation.<sup>18</sup> The change of the secondary structure of the protein after infiltration in COF-OMe was also confirmed by circular dichroism spectroscopic analysis, as detailed in Figure S24.

To demonstrate the effect of pore structures on the performance of the infiltrated enzymes, the catalytic activity of lipase@POP-OMe was evaluated. After 10 min, it afforded a 1-phenylethyl acetate yield of 16%, which is less than half as much achieved by employing lipase@COF-OMe. A similar trend was also seen for lipase@COF-V and lipase@POP-V, which gave rise to 26% and 11% conversions of 1-phenylethanol, respectively. Considering that POP-OMe and POP-V have the same chemical composition as that of COF-OMe and COF-V, the primary reason behind the huge disparity in activities between COF-based and POP-based biocomposites should stem from the pore structures. One possible explanation is that the COFs provide continuous nanometer-scale channels which assist in proper orientation of the enzyme molecule due to hydrophobic interactions. Such orientation of the enzyme molecules may decrease the mass transfer limitation of substrates and thus increases the reaction conversion, compared to the randomly orientated ones. In contrast, due to the irregular pores of POPs, part of the enzymes were plunged in small pores, which are inaccessible to the reagents, while some of them may aggregate in the relatively larger pores. All of this would compromise the enzymatic activity, thus underscoring the superiority of using COFs as a new type of platform for enzyme immobilization in comparison with their amorphous analogues.

As demonstrated above, lipase PS encapsulated in hydrophobic COFs exhibits high activities in nonpolar organic solvents, however, a polar solvent is often required because of substrate solubility issues. Therefore, enhancing the activity of lipase in polar solvents is profitable, which is believed to greatly expand the utility of lipase in organic synthesis. We envision that the strong hydrophobic interactions between the COFs and the enzymes are beneficial for sustaining the enzymatic

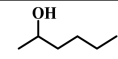
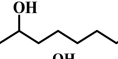
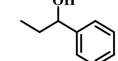
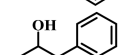
performance under polar solvents. To test this assumption, the reactions were carried out using acetonitrile as the solvent (Figure 5a). It is noteworthy that the activities of lipase@COF-OMe and lipase@COF-V in acetonitrile were still remarkable, although inferior to those using hexane as the reaction media, giving 45% and 42% conversions of 1-phenylethanol, respectively, after 12 h. Under identical conditions, lipase@COF-OH and lipase@COF-ONa only showed 22% and 7% conversions, respectively, while lipase@POP-OMe and lipase@POP-V resulted in 28% and 23% conversions, respectively, and no detectable product yields were observed for free lipase PS, lipase@MCM-41, or lipase@PCN-128y. In addition to acetonitrile, higher activities were also observed for lipase@COF-OMe relative to that of free lipase PS in other polar systems such as water or water/DMSO mixture solutions (Table S3). These results indicate that the hydrophobic COF channels are ideal for the accommodation of lipase PS, greatly improving its tolerance to the solvent.

Given the high enzyme uptake capacity and superior catalytic performance of the encapsulated enzymes, COF-OMe was thus chosen as a representative sample for further studies. In nature, biomineral coatings are universally used to protect tissue from its surrounding environment. This motivated us to examine whether COF walls could provide a similar shield that would enable the infiltrated enzymes to withstand extreme conditions (for example, high temperature or stringent reaction media) that would normally lead to the denaturation of the enzymes. Success in this endeavor would significantly increase the potential for the applications of enzymes where enhanced thermal stability, tolerance to reaction media, or extended shelf-life is required.<sup>24</sup> To assess the shield effect of the COF host on the enzyme's thermal stability, we measured the extent of kinetic resolution of racemic 1-phenylethanol with vinyl acetate achieved over free lipase PS versus lipase@COF-OMe after incubation at a range of temperatures and times. Both show thermal stability when they were incubated below 60 °C for 12 h. However, the incubation of free lipase PS at 100 °C for 3 h results in an obvious loss of enzymatic activity for lipase PS, as evidenced by a clear drop of 1-phenylethanol conversion from 29% to 18% after 15 h reaction time. In contrast, lipase@COF-OMe well retained its performance, giving rise to a comparable conversion of 1-phenylethanol in relation to the fresh catalyst (34% vs 33%) after 10 min (Figure 5b). When we further increased the incubation temperature to 120 °C and prolonged the treatment time to 24 h, lipase@COF-OMe still showed remarkable stability, retaining around 75% of its original activity (25% vs 34%). This compares with only 2% conversion for an analogous experiment of the free enzyme. In a further set of experiments, the same systems were immersed in benzonitrile at 120 °C for 1 h. The free enzyme completely lost activity, while the COF biocomposite achieved a 37% and 48% conversion after 30 min and 1 h, respectively, demonstrating again the extraordinary protective properties of the COF walls (Figure 5b). These findings suggest that the confined space of COF channels may provide the stability necessary for the enzymes to retain their performance in rigorous conditions. In this sense, to assess the importance of the well-defined pore channels in preserving catalytic function of the enzyme, the tolerance of lipase@POP-OMe against hot benzonitrile was evaluated. As shown in Figure 5c, the drop in activity of lipase@POP-OMe is lower compared to free lipase PS, indicating a certain degree of stabilization. However, the activity drop is greater compared to lipase@COF-OMe. This

indicates that the protection against enzyme deactivation is more pronounced for COF-OMe, possibly because the well-defined yet relatively small pore size can isolate the protein molecules and prevent their aggregation and thereby deactivation. Encouraged by the greater stability of lipase PS after encapsulation in COF-OMe, we sought to investigate the recyclability of lipase@COF-OMe, a significant performance metric for practical processes. Impressively, the catalyst could be recycled at least 6 times without a drop in product yield and enantioselectivity, indicating its excellent stability. Liquid  $^1\text{H}$  NMR results indicate that no leaching of the enzyme was found during the recycling, due to the strong interactions between the COF and the enzyme as well as the low solubility of the enzyme in hexane. In addition, a negligibly changed IR spectrum of the recycled catalyst compared to that of the fresh catalyst suggests the maintenance of enzyme conformation (Figure S25). Moreover, the crystallinity and porosity of the composite were retained during the catalytic process, as proven by the comparable PXRD pattern and surface area of the reused lipase@COF-OMe relative to the fresh catalyst (Figure S26). In contrast, the activity of free lipase PS was reduced by more than 60% during the second use (29% vs 11%, Figure 5d). To further demonstrate the long-term durability of lipase@COF-OMe, relatively large-scale catalysis experiments were conducted by employing 1-phenylethanol (2.0 g) and catalyst (2.5 mg). After 48 h, a 48% 1-phenylethyl acetate yield was observed, and outstandingly, similar values (47%) can be afforded by the recycled catalyst, thus indicating the robustness of the catalyst.

Having established the efficiency of lipase@COF-OMe in the kinetic resolution of 1-phenylethanol, we then studied the scope of this catalyst for the kinetic resolution of other secondary alcohols with vinyl acetate and found that it is broadly applicable (Table 1). Alkyl-substituted alcohols, such as 2-octanol and 2-hexanol, were superb substrates and underwent efficient resolution with high enantiomer excess (ee) values. Other aromatic alcohols, such as 1-phenyl-1-propanol and 1-phenyl-2-propanol, were resolved with lower activity due to the high steric hindrance, but highly enantiomerically enriched

**Table 1.** Lipase@COF-OMe-Catalyzed Kinetic Resolution of Secondary Alcohols with Vinyl Acetate<sup>a</sup>

Entry	Racemic alcohol	Time (h)	Yield (%)
1		0.5	>49
2		0.5	>49
3		2	48
4		2	47

<sup>a</sup>Reaction conditions: Alcohol (0.25 mmol), vinyl acetate (0.75 mmol), hexane (1.2 mL), lipase@COF-OMe (2.5 mg), and 45 °C. All the reactions gave ee values higher than 99.5%, as determined by HPLC, and the theoretical yield is 50%.

products could still be obtained in useful yields by prolonging the reaction time.

To yield high volumetric activity for a higher productivity and space-time yield and to examine the enzyme accessibility after immobilization, composites with different enzyme loadings were prepared and tested for kinetic resolution of racemic 1-phenylethanol with vinyl acetate. As shown in Figure S27, volumetric activity of the resultant biocomposites increased with the increment of the concentration of enzyme buffer aqueous solutions from 10 mg mL<sup>-1</sup> to 35 mg mL<sup>-1</sup> (the enzyme loading amount increased from 0.21 to 1.08, Table S4, Figures S27–S29), affording conversions of 1-phenylethanol from 19% to 42% after 10 min. However, further increasing the loading by treatment with the 40 mg mL<sup>-1</sup> enzyme stock solution did not result in increased activity (41%). This may be due to high enzyme loading partly blocking the reactants to access the enzymes situated in the channels of the COF.

## CONCLUSION

In summary, we have demonstrated for the first time that due to the unique mesoporous structure and the tunable surface chemistry, COFs provided both high affinity for enzyme loading and a favored microenvironment that enhanced the enzymatic performance better than in other types of porous materials reported. This proven enhancement showed their utility with orders of magnitude higher catalytic activities compared to free enzymes and biocomposites made from other types of porous materials, in addition to easy recycling of the catalyst and greatly improved stability. This investigation opens new opportunities for developing COFs as a promising type of host material for the immobilization and stabilization of enzymes in a wide range of applications.

## ASSOCIATED CONTENT

### Supporting Information

The Supporting Information is available free of charge on the ACS Publications website at DOI: 10.1021/jacs.7b10642.

Material synthesis; characterization details; IR, SEM, and NMR; and supporting figures (PDF)

## AUTHOR INFORMATION

### Corresponding Authors

\*sqma@usf.edu

\*hyhuang@cycu.edu.tw

### ORCID

Jason Perman: 0000-0003-4894-3561

Hsi-Ya Huang: 0000-0002-3020-7622

Feng-Shou Xiao: 0000-0001-9744-3067

Shengqian Ma: 0000-0002-1897-7069

### Author Contributions

<sup>||</sup>These authors contributed equally.

### Notes

The authors declare no competing financial interest.

## ACKNOWLEDGMENTS

The authors acknowledge the National Science Foundation (DMR-1352065) and the University of South Florida for financial support of this work. Partial financial support from the Ministry of Science and Technology of Taiwan (MOST 104-2113-M-033-003-MY3) and Chung Yuan Christian University (CYF and HYH) and National Natural Science Foundation of

China (21720102001, SW and FSX) is also acknowledged. We are grateful to Professor Bao-Tsan Ko at National Chung Hsing University, Taiwan, for the assistance in the CLSM experiments.

## REFERENCES

- (1) (a) Schmid, A.; Dordick, J. S.; Hauer, B.; Kiener, A.; Wubbolts, M.; Witholt, B. *Nature* **2001**, *409*, 258–268. (b) Schoemaker, H. E.; Mink, D.; Wubbolts, M. G. *Science* **2003**, *299*, 1694–1697. (c) Dicosimo, R.; McAuliffe, J.; Poulouse, A. J.; Bohlmann, G. *Chem. Soc. Rev.* **2013**, *42*, 6437–6474.
- (2) (a) Lian, X.; Fang, Y.; Joseph, E.; Wang, Q.; Li, J.; Banerjee, S.; Lollar, C.; Wang, X.; Zhou, H.-C. *Chem. Soc. Rev.* **2017**, *46*, 3386–3401. (b) Hanefeld, U.; Gardossi, L.; Magner, E. *Chem. Soc. Rev.* **2009**, *38*, 453–468. (c) Zhou, Z.; Hartmann, M. *Chem. Soc. Rev.* **2013**, *42*, 3894–3912. (d) Cao, L. Q. *Curr. Opin. Chem. Biol.* **2005**, *9*, 217–226. (e) Bornscheuer, U. T. *Angew. Chem., Int. Ed.* **2003**, *42*, 3336–3337. (f) Sheldon, R. A. *Adv. Synth. Catal.* **2007**, *349*, 1289–1307. (g) Chen, Y.; Ma, S. *Dalton Trans.* **2016**, *45*, 9744–9753. (h) Hou, C.; Wang, Y.; Ding, Q.; Jiang, L.; Li, M.; Zhu, W.; Pan, D.; Zhu, H.; Liu, M. *Nanoscale* **2015**, *7*, 18770–18779. (i) Shieh, F.-K.; Wang, S.-C.; Yen, C.-I.; Wu, C.-C.; Dutta, S.; Chou, L.-Y.; Morabito, J. V.; Hu, P.; Hsu, M.-H.; Wu, K. C.-W.; Tsung, C.-K. *J. Am. Chem. Soc.* **2015**, *137*, 4276–4279.
- (3) (a) Li, P.; Moon, S.-Y.; Guelta, M. A.; Harvey, S. P.; Hupp, J. T.; Farha, O. K. *J. Am. Chem. Soc.* **2016**, *138*, 8052–8055. (b) Feng, D.; Liu, T.-F.; Su, J.; Bosch, M.; Wei, Z.; Wan, W.; Yuan, D.; Chen, Y.-P.; Wang, X.; Wang, K.; Lian, X.; Gu, Z.-Y.; Park, J.; Zou, X.; Zhou, H.-C. *Nat. Commun.* **2015**, *6*, 5979. (c) Garcia-Galan, C.; Berenguer-Murcia, Á.; Fernandez-Lafuente, R.; Rodrigues, E. C. *Adv. Synth. Catal.* **2011**, *353*, 2885–2904. (d) Torres-Salas, P.; del Monte-Martinez, A.; Cutiño-Avila, B.; Rodriguez-Colinas, B.; Alcalde, M.; Ballesteros, A. O.; Plou, F. J. *Adv. Mater.* **2011**, *23*, 5275–5282.
- (4) (a) Bae, J.-S.; Jeon, E.; Moon, S.-Y.; Oh, W.; Han, S.-Y.; Lee, J. H.; Yang, S. Y.; Kim, D.-M.; Park, J.-W. *Angew. Chem., Int. Ed.* **2016**, *55*, 11495–11498. (b) Fried, D. I.; Brieler, F. J.; Fröba, M. *ChemCatChem* **2013**, *5*, 862–884. (c) Li, P.; Modica, J. A.; Howarth, A. J.; Vargas, L. E.; Moghadam, P. Z.; Snurr, R. Q.; Mrksich, M.; Hupp, J. T.; Farha, O. K. *Chem.* **2016**, *1*, 154–169.
- (5) (a) Hudson, S.; Cooney, J.; Magner, E. *Angew. Chem., Int. Ed.* **2008**, *47*, 8582–8594. (b) Gill, I.; Ballesteros, A. *J. Am. Chem. Soc.* **1998**, *120*, 8587–8598. (c) Hartmann, M. *Chem. Mater.* **2005**, *17*, 4577–4593. (d) Han, Y.; Lee, S. S.; Ying, J. Y. *Chem. Mater.* **2006**, *18*, 643–649. (e) Lei, C.; Shin, Y.; Liu, J.; Ackerman, E. J. *J. Am. Chem. Soc.* **2002**, *124*, 11242–11243. (f) Lee, C.-H.; Lin, T.-S.; Mou, C.-Y. *Nano Today* **2009**, *4*, 165–179.
- (6) (a) Doonan, C.; Riccò, R.; Liang, K.; Bradshaw, D.; Falcaro, P. *Acc. Chem. Res.* **2017**, *50*, 1423–1432. (b) Gkaniatsou, E.; Sicard, C.; Ricoux, R.; Mahy, J.-P.; Steunou, N.; Serre, C. *Mater. Horiz.* **2017**, *4*, 55–63. (c) Deng, H.; Grunder, S.; Cordova, K. E.; Valente, C.; Furukawa, H.; Hmadeh, M.; Gándara, F.; Whalley, A. C.; Liu, Z.; Asahina, S.; Kazumori, H.; O’Keeffe, M.; Terasaki, O.; Stoddart, J. F.; Yaghi, O. M. *Science* **2012**, *336*, 1018–1023. (d) Jung, S.; Park, S. *ACS Catal.* **2017**, *7*, 438–442. (e) Jeong, G.-Y.; Ricco, R.; Liang, K.; Ludwig, J.; Kim, J.-O.; Falcaro, P.; Kim, D.-P. *Chem. Mater.* **2015**, *27*, 7903–7909. (f) Huo, J.; Sigalat-Aguilera, J.; El-Hankari, S.; Bradshaw, D. *Chem. Sci.* **2015**, *6*, 1938–1943. (g) Lykourinou, V.; Chen, Y.; Wang, X.-S.; Meng, L.; Hoang, T.; Ming, L.-J.; Musselman, R. L.; Ma, S. *J. Am. Chem. Soc.* **2011**, *133*, 10382–10385. (h) Majewski, M. B.; Howarth, A. J.; Li, P.; Wasielewski, M. J.; Hupp, J. T.; Farha, O. K. *CrystEngComm* **2017**, *19*, 4082–4091.
- (7) Mitra, S.; Sasmal, H. S.; Kundu, T.; Kandambeth, S.; Illath, K.; Díaz, D. D.; Banerjee, R. *J. Am. Chem. Soc.* **2017**, *139*, 4513–4520.
- (8) (a) Côté, A. P.; Benin, A. I.; Ockwig, N. W.; O’Keeffe, M.; Matzger, A. J.; Yaghi, O. M. *Science* **2005**, *310*, 1166–1170. (b) Jin, Y.; Hu, Y.; Zhang, W. *Nat. Rev. Chem.* **2017**, *1*, 0056. (c) Feng, X.; Ding, X.; Jiang, D. *Chem. Soc. Rev.* **2012**, *41*, 6010–6022. (d) Ding, S.-Y.; Wang, W. *Chem. Soc. Rev.* **2013**, *42*, 548–568. (e) Pang, Z.-F.; Xu, S.-Q.; Zhou, T.-Y.; Liang, R.-R.; Zhan, T.-G.; Zhao, X. *J. Am. Chem. Soc.* **2016**, *138*, 4710–4713. (f) Rao, M. R.; Fang, Y.; Feyter, S. D.; Perepichka, D. F. *J. Am. Chem. Soc.* **2017**, *139*, 2421–2427. (g) Lin, G.; Ding, H.; Yuan, D.; Wang, B.; Wang, C. *J. Am. Chem. Soc.* **2016**, *138*, 3302–3305. (h) Kandambeth, S.; Mallick, A.; Lukose, B.; Mane, M. V.; Heine, T.; Banerjee, R. *J. Am. Chem. Soc.* **2012**, *134*, 19524–19527. (i) Bisbey, R. P.; Dichtel, W. R. *ACS Cent. Sci.* **2017**, *3*, 533–543.
- (9) (a) Du, Y.; Yang, H.; Whiteley, J. M.; Wan, S.; Jin, Y.; Lee, S.-H.; Zhang, W. *Angew. Chem., Int. Ed.* **2016**, *55*, 1737–1741. (b) Zeng, Y.; Zou, R.; Zhao, Y. *Adv. Mater.* **2016**, *28*, 2855–2873. (c) Baldwin, L. A.; Crowe, J. W.; Pyles, D. A.; McGrier, P. L. *J. Am. Chem. Soc.* **2016**, *138*, 15134–15137. (d) Pramudya, Y.; Mendoza-Cortes, J. L. *J. Am. Chem. Soc.* **2016**, *138*, 15204–15313.
- (10) (a) Lin, S.; Diercks, C. S.; Zhang, Y.-B.; Kornienko, N.; Nichols, E. M.; Zhao, Y.; Paris, A. R.; Kim, D.; Yang, P.; Yaghi, O. M.; Chang, C. J. *Science* **2015**, *349*, 1208–1213. (b) Ding, S.-Y.; Gao, J.; Wang, Q.; Zhang, Y.; Song, W.-G.; Su, C.-Y.; Wang, W. *J. Am. Chem. Soc.* **2011**, *133*, 19816–19822. (c) Vyas, V. S.; Haase, F.; Stegbauer, L.; Savasci, G.; Podjaski, F.; Ochsenfeld, C.; Lotsch, B. V. *Nat. Commun.* **2015**, *6*, 8508. (d) Sun, Q.; Aguila, B.; Perman, J. A.; Nguyen, N.; Ma, S. *J. Am. Chem. Soc.* **2016**, *138*, 15790–15796. (e) Wang, X.; Han, X.; Zhang, J.; Wu, X.; Liu, Y.; Cui, Y. *J. Am. Chem. Soc.* **2016**, *138*, 12332–12335.
- (11) (a) Bertrand, G. H. V.; Michaelis, V. K.; Ong, T.-C.; Griffin, R. G.; Dincă, M. *Proc. Natl. Acad. Sci. U. S. A.* **2013**, *110*, 4923–4928. (b) Calik, M.; Auras, F.; Salonen, L. M.; Bader, K.; Grill, I.; Handloser, M.; Medina, D. D.; Dogru, M.; Löbermann, F.; Trauner, D.; Hartschuh, A.; Bein, T. *J. Am. Chem. Soc.* **2014**, *136*, 17802–17807.
- (12) Ma, H.; Liu, B.; Li, B.; Zhang, L.; Li, Y.-G.; Tan, H.-Q.; Zang, H.-Y.; Zhu, G. *J. Am. Chem. Soc.* **2016**, *138*, 5897–5903.
- (13) (a) Sun, Q.; Aguila, B.; Perman, J.; Earl, L.; Abney, C.; Cheng, Y.; Wei, H.; Nguyen, N.; Wojtas, L.; Ma, S. *J. Am. Chem. Soc.* **2017**, *139*, 2786–2793. (b) Huang, N.; Zhai, L.; Xu, H.; Jiang, D. *J. Am. Chem. Soc.* **2017**, *139*, 2428–2434.
- (14) (a) Fang, Q.; Wang, J.; Gu, S.; Kaspar, R. B.; Zhuang, Z.; Zheng, J.; Guo, H.; Qiu, S.; Yan, Y. *J. Am. Chem. Soc.* **2015**, *137*, 8352–8355. (b) Kandambeth, S.; Venkatesh, V.; Shinde, D. B.; Kumari, S.; Halder, A.; Verma, S.; Banerjee, R. *Nat. Commun.* **2015**, *6*, 6786. (c) Wang, S.; Wang, Q.; Shao, P.; Han, Y.; Gao, X.; Ma, L.; Yuan, S.; Ma, X.; Zhou, J.; Feng, X.; Wang, B. *J. Am. Chem. Soc.* **2017**, *139*, 4258–4261. (d) Ning, G.-H.; Chen, Z.; Gao, Q.; Tang, W.; Chen, Z.; Liu, C.; Tian, B.; Li, X.; Loh, K. P. *J. Am. Chem. Soc.* **2017**, *139*, 8897–8904. (e) Peng, Y.; Huang, Y.; Zhu, Y.; Chen, B.; Wang, L.; Lai, Z.; Zhang, Z.; Zhao, M.; Tan, C.; Yang, N.; Shao, F.; Han, Y.; Zhang, H. *J. Am. Chem. Soc.* **2017**, *139*, 8698–8704.
- (15) (a) Wu, Q.; Soni, P.; Reetz, M. T. *J. Am. Chem. Soc.* **2013**, *135*, 1872–1881. (b) Svedendahl, M.; Hult, K.; Berglund, P. *J. Am. Chem. Soc.* **2005**, *127*, 17988–17989. (c) Dyal, A.; Loos, K.; Noto, M.; Chang, S. W.; Spagnoli, C.; Shafi, K. V. P. M.; Ulman, A.; Cowman, M.; Cross, R. A. *J. Am. Chem. Soc.* **2003**, *125*, 1684–1685. (d) Liu, W.-L.; Yang, N.-S.; Chen, Y.-T.; Lirio, S.; Wu, C.-Y.; Lin, C.-H.; Huang, H.-Y. *Chem. - Eur. J.* **2015**, *21*, 115–119. (e) Bhattacharyya, M. S.; Hiwale, P.; Piras, M.; Medda, L.; Steri, D.; Piludu, M.; Salis, A.; Monduzzi, M. *J. Phys. Chem. C* **2010**, *114*, 19928–19934.
- (16) He, H.; Han, H.; Shi, H.; Tian, Y.; Sun, F.; Song, Y.; Li, Q.; Zhu, G. *ACS Appl. Mater. Interfaces* **2016**, *8*, 24517–24524.
- (17) Xu, H.; Gao, J.; Jiang, D. *Nat. Chem.* **2015**, *7*, 905–912.
- (18) Reis, P.; Witula, T.; Holmberg, K. *Microporous Mesoporous Mater.* **2008**, *110*, 355–362.
- (19) Chen, Y.; Lykourinou, V.; Vetroville, C.; Hoang, T.; Ming, L.-J.; Larsen, R. W.; Ma, S. *J. Am. Chem. Soc.* **2012**, *134*, 13188–13191.
- (20) Kresge, C. T.; Leonowicz, M. E.; Roth, W. J.; Vartuli, J. C.; Beck, J. S. *Nature* **1992**, *359*, 710–712.
- (21) Zhang, Q.; Su, J.; Feng, D.; Wei, Z.; Zou, X.; Zhou, H.-C. *J. Am. Chem. Soc.* **2015**, *137*, 10064–10067.
- (22) (a) Liu, J.; Bai, S.; Jin, Q.; Zhong, H.; Li, C.; Yang, Q. *Langmuir* **2012**, *28*, 9788–9796. (b) Chen, C. S.; Wu, S. H.; Girdaukas, G.; Sih, C. J. *J. Am. Chem. Soc.* **1987**, *109*, 2812–2817.
- (23) (a) Schmid, R. D.; Verger, R. *Angew. Chem., Int. Ed.* **1998**, *37*, 1608–1633. (b) Manoel, E. A.; dos Santos, J. C.S.; Freire, D. M.G.;



Rueda, N.; Fernandez-Lafuente, R. *Enzyme Microb. Technol.* **2015**, *71*, 53–57.

(24) (a) Liao, F.-S.; Lo, W.-S.; Hsu, Y.-S.; Wu, C.-C.; Wang, S.-C.; Shieh, F.-K.; Morabito, J. V.; Chou, L.-Y.; Wu, K. C.-W.; Tsung, C.-K. *J. Am. Chem. Soc.* **2017**, *139*, 6530–6533. (b) Liang, K.; Ricco, R.; Doherty, C. M.; Styles, M. J.; Bell, S.; Kirby, N.; Mudie, S.; Haylock, D.; Hill, A. J.; Doonan, C. J.; Falcaro, P. *Nat. Commun.* **2015**, *6*, 7240. (c) Lyu, F.; Zhang, Y.; Zare, R. N.; Ge, J.; Liu, Z. *Nano Lett.* **2014**, *14*, 5761–5765.